Scientific Research and Essays Vol. 5(13), pp. 1702-1712, 4 July, 2010
Available online at http://www.academicjournals.org/SRE
ISSN 1992-2248 ©2010 Academic Journals

Full Length Research Paper

Effect of upstream crest length on flow characteristics and discharge capacity of triangular labyrinth side weirs

Nihat Kaya

Civil Engineering Department, Faculty of Engineering, Firat University, 23119, Elazig, Turkey. E-mail: nkaya@firat.edu.tr.

Accepted 3 June, 2010

A series of laboratory experiments were performed within this study in order to investigate the hydraulic characteristics and the discharge capacity of sharp-crested triangular labyrinth side weirs with various upstream crest lengths. To conduct the experiment series, twenty seven different labyrinth side weir models having triangular plan view that are manufactured from steel were tested in the laboratory flume. A labyrinth weir is an overflow weir that is folded in plan view to provide a longer total effective length for a given overall weir width. To estimate the outflow over a side weir, the discharge coefficient in the side weir equation needs to be determined. A comprehensive laboratory study including 679 tests was conducted to determine the discharge coefficient of the side weirs. It was found that the discharge coefficient of triangular labyrinth side weirs was higher than that of classical side weirs. In addition, reliable equations to calculate the discharge coefficient of side weirs are presented.

Key words: Side weir, discharge coefficient, labyrinth weir, hydraulic structure, open channel flow.

INTRODUCTION

A side weir is a hydraulic control structure used to divert flow from a main channel into a side channel when the water level in the main channel exceeds a specified limit. As the name suggest, the structure is normally located by the side of the channel and water discharges over it freely under gravity in the same way as for conventional weirs. The most common function of a side weir is to remove flow from a channel in order to prevent the downstream flow capacity of the channel being exceeded. It is usual required that this function should be achievable without a large increase in the water level in the parent channel. Hence, the side weir is often considered as a means of limiting water level but, in fact, this is generally a secondary requirement of the structure. Typical examples of side weirs include (May, et al. 2003):

1. A flood overflow structure in a river channel, usually designed to divert excess flow into an off-stream storage reservoir or flood bypass channel, thereby protecting downstream infrastructure from flooding.
2. A storm-water overflow in a combined sewer, designed to divert excess flow that would otherwise overload the sewer downstream.
3. A storm–water overflow in the approach channel to a wastewater treatment works, to ensure that the capacity of the works is not exceeded.

A labyrinth weir (or spillway) is an overflow weir to provide a longer total effective length for a given overall spillway width. A labyrinth weir has advantages compared to the straight overflow weir and the standard ogee crest. The total length of the labyrinth weir is typically three to five greater than the spillway width. Its capacity varies with head and is typically about twice that of a standard weir or overflow crest of the same width (Tullis et al., 1995).

A review of previous studies indicated that rectangular sharp-crested side weirs have been investigated extensively, including work by Ackers (1957), Collings (1957), Frazer (1957), Subramanya and Awasthy (1972),

El-Khashab and Smith (1976), Uyumaz and Muslu (1985), Helweg (1991) and, Agaccioglu and Yüksel (1998). Borghei et al. (1999) studied the discharge coefficient for sharp-crested side weirs in subcritical flow, and developed an equation for the discharge coefficient of sharp-crested rectangular side weirs. Also, in order to study the variation of the discharge coefficient along side weirs, Swamee et al. (1994) used an elementary analysis approach to estimate the discharge in smooth side weirs through an elementary strip along the side weir. The hydraulic behavior and the discharge coefficient of different types of weirs have been studied by many researchers, including: Nandesomoorthy and Thomson (1972), Singh et al. (1994), Yu-tech (1972), Cheong (1991), and others. Ranga et al. (1979) investigated the discharge coefficient of a broad-crested rectangular side weir, based on the width of the main channel, Froude number and head/weir width ratio. Kumar and Pathak (1987) investigated the discharge coefficient of sharp and broad-crested triangular side weirs. Ghodsian (2003) studied supercritical flow in rectangular side weirs. Cosar and Agaccioglu (2004) studied the discharge coefficient of a triangular side weir both on straight and curved channels. Aghayari et al. (2009) investigated experimentally the effect of height, width and side weir crest slope on the spatial discharge coefficient over broad-crested inclined side weirs under subcritical flow conditions in a rectangular channel.

The flow over a side weir falls within the category of spatially varied flow. The existing studies deal mainly with the application of energy principle in the analysis of side weir flow. The concept of constant specific energy (De Marchi, 1934) is often adopted for studying the flow characteristics of these weirs (Emiroglu et al. 2010a, b; Emiroglu et al. 2007; Bilhan et al. 2010; Singh et al., 1994; Hager, 1987, 1994; Subramanya and Awasthy, 1972).

There is considerable interest, particularly in rectangular side weirs. De Marchi (1934) was one of the first researchers to provide equations for flow over side weirs. Considering the discharge *dQ* through an elementary strip of length *dx* along the side weir in a rectangular main channel as a De Marchi equation, one gets:

$$q = -\frac{dQ}{dx} = \frac{2}{3} C_d \sqrt{2g}\,[h-p]^{3/2} \quad (1)$$

where *Q* is the discharge in the main channel, *s* is the distance from the beginning of the side weir, *dQ/dx* (or *q*) is the spill discharge per unit length of the side opening, *g* is acceleration due to gravity, *p* is crest height of the side weir, *h* is the depth of flow measured from the channel bottom along the channel centerline, and C_d is the discharge coefficient (De Marchi coefficient) of the side weir. Thus, the side weir discharge equation can be written as:

$$Q_w = \frac{2}{3} C_d\, L\sqrt{2g}\,[h-p]^{3/2} \quad (2)$$

in which total flow over side weir Q_w is in m^3/s, the discharge coefficient C_d is dimensionless, the width of side-weir *L* is in meters, and *h* and *p* are in meters (Figure 1). This equation is usually used for flow over flat, broad-crested, quarter-round, half-round, and nappe (ogee) profile weirs.

Some of the proposed formulas for the discharge coefficient of the rectangular side weirs (Figure 1a, b) are as follows:

$$C_d = 0.864\left(\frac{1-\mathbf{F}_1^2}{2+\mathbf{F}_1^2}\right)^{0.5} \text{ Subramanya and Awasthy (1972)} \quad (3)$$

$$C_d = 0.81 - 0.6\mathbf{F}_1 \text{ Ranga et al. (1979)} \quad (4)$$

$$C_d = 0.485\left(\frac{2+\mathbf{F}_1^2}{2+\mathbf{F}_1^2}\right)^{0.5} \text{ Hager (1987)} \quad (5)$$

$$C_d = 0.7 - 0.48\mathbf{F}_1 - 0.3\frac{p}{h_1} + 0.06\frac{L}{b} \text{ Borghei et al. (1999)} \quad (6)$$

Most of presented equations for C_d depend on Froude number. Most researchers have concentrated on investigating rectangular and triangular side weirs in straight channels. Kumar and Pathak (1987) investigated the variation of discharge coefficient for a sharp-crested triangular side weir having 60°, 90° and 120° apex angles, and presented equations depending only on the Froude number and the apex angle. Hager (1994) studied supercritical flow in circular-shaped side weirs. Oliveto et al. (2001) studied the hydraulic characteristics of side weirs in circular channels when flow along the side weir is supercritical. As mentioned above, the most common type of side weir is rectangular. Moreover, triangular and circular types are also used in hydraulic and environmental engineering applications.

Emiroglu et al. (2010a) studied the discharge coefficient of sharp-crested triangular labyrinth side weirs on a straight channel. Dimensionless parameters for triangular labyrinth side weir discharge coefficient on a straight channel given by them are:

$$C_d = f(\mathbf{F}_1, L/b, L/s, p/h_1, \theta, \psi) \quad (7)$$

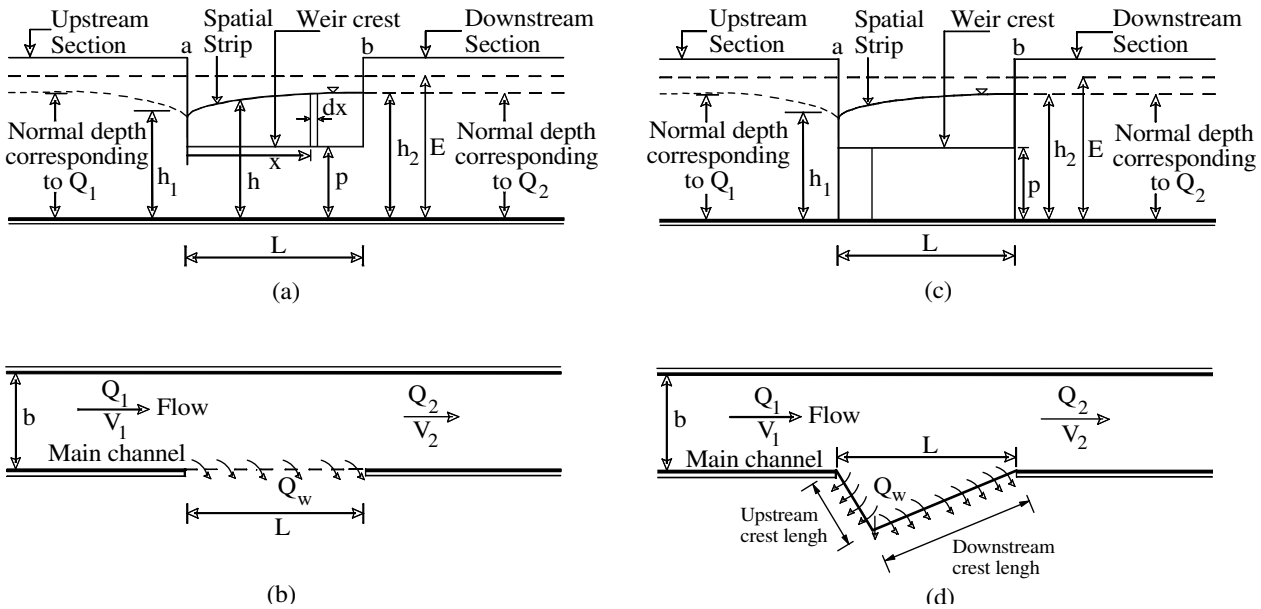

Figure 1. Definition sketch of subcritical flow over a rectangular and labyrinth side weir tested. (a) Longitudinal cross-section for the rectangular side weir, (b) Plan for the rectangular side weir, (c) Longitudinal cross-section for the labyrinth side weir tested, (d) Plan for the labyrinth side weir tested.

in which, $\mathbf{F}_1$ is the upstream Froude number at the beginning of the side weir in the main channel, C_d is the discharge coefficient (De Marchi coefficient), p is the crest height of the side weir, L is the width (length) of the side weir; b is the width of the main channel; s is the overflow length of the side weir, h_1 is the depth of flow at the upstream end of the side weir in the main channel centerline. The dimensionless parameters were explained as follows: L/b is the dimensionless weir length (width), L/s is the dimensionless effective side weir length, p/h_1 *is* the dimensionless weir crest height, θ is the included angle of the triangular labyrinth side weir.

The water nape deviation or deflection angle ψ is defined as the deflection of the side weir nape from the water surface toward the weir side, and is given as follows (Subramanya and Awasthy, 1972):

$$\sin\psi = \sqrt{1-(\frac{V_1}{V_s})^2} \qquad (8)$$

in which, V_s is velocity of flow dQ_s over the brink. According to equation 8, ψ takes different values for each fluid particle and varies with Froude number, which changes along the side weir due to spilling over the side weir. The deviation angle increases towards the weir side when the Froude number in the main channel decreases towards the downstream direction. El Khashab (1975) also mentioned that the dimensionless length of the side weir (L/b) includes the effect of the deviation angle on the discharge coefficient. Therefore, the deviation angle ψ is not included in the side weir discharge coefficient equations in the literature.

Emiroglu et al. (2010a) obtained the following results regarding the labyrinth side weir discharge coefficient:

1. Discharge coefficient of the labyrinth side weir is 1.5 - 4.5 times higher than that of the rectangular side weir.
2. The discharge coefficient C_d increases when L/b ratio increases. A decrease in the labyrinth weir included angle θ which causes a considerable increase in C_d, due to increase in the overflow length. The labyrinth side weir with $\theta = 45°$ has the greatest C_d values among the weir included angles that were tested.
3. The following proposed equation for C_d, De Marchi coefficient, for subcritical flow can be used reliably:

$$C_d = \left[18.6 - 23.535\left(\frac{L}{b}\right)^{0.012} + 6.769\left(\frac{L}{s}\right)^{0.112} - 0.502\left(\frac{p}{h_1}\right)^{4.024} + 0.094.\sin\theta - 0.393\,\mathbf{F}_1^{2.155}\right]^{-1.431} \qquad (9)$$

As mentioned above, side weirs are used widely in order to

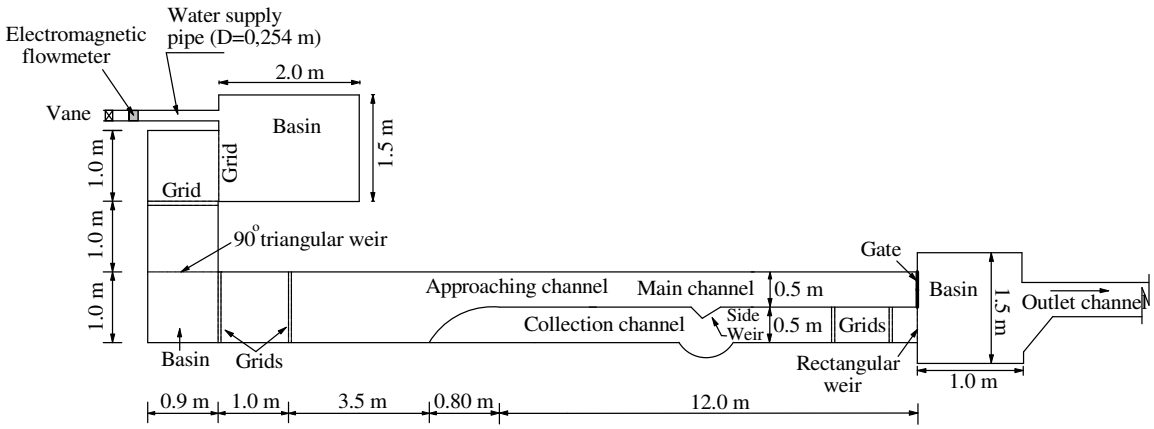

Figure 2. Experimental arrangement.

divert flows from rivers, canals, sewers and reservoirs. However, the hydraulic behavior of this type of weir is complex and difficult to predict accurately by simple methods. This paper investigates the effect of upstream crest length on flow characteristics and discharge coefficient of triangular labyrinth side weirs. The present study was conducted for subcritical flow regime, and stable flow conditions and free overflow conditions.

EXPERIMENTAL SETUP AND EXPERIMENTS

Experiments were conducted at the Hydraulic Laboratory of Firat University, Elazig, Turkey. A schematic representation of the experimental set-up is shown in Figure 2. The experimental set-up consisted of a main channel and a discharge collection channel. The main channel was 12 m long and the bed had a rectangular cross-section. The main channel was 0.50 m wide, 0.50 m deep, and has a 0.001 bed slope. The channel was constructed from a smooth, horizontal, well-painted steel bed with vertical glass sidewalls. A sluice gate was fitted at the end of the main channel in order to control the depth of flow. The collection channel was 0.50 m wide and 0.70 m deep, and was situated parallel to the main channel. The width of the collection channel across the side weir was 1.3 m and constructed in a circular shape, to provide free overflow conditions. A rectangular weir was placed at the end of the collection channel, in order to measure the discharge of the side weir. A Mitutoyo digital point gauge with ± 0.01 mm sensitivity was fixed at a location 0.40 m from the weir. Semi-elliptical side weirs were produced from steel plates, which had sharp edges and were fully aerated. These were installed flush with the main channel wall.

Water was supplied to the main channel, through a supply pipe, from a sump and the flow was controlled by a gate valve. The discharge was measured to an accuracy ± 0.01 L/s, by means of a Siemens electromagnetic flow-meter installed in the supply line. The results were compared by a calibrated 90° V-notched weir. The overflow rate was measured by a calibrated standard rectangular weir, located at the downstream end of the collection channel.

Water depth measurements were conducted using the digital point gauges at the side weir region, along the channel centerline and the weir-side of the main. Water surface measurements were made by using a special type of measurement car, which can move in both directions on a rail.

Experiments were conducted at subcritical flow, stable flow conditions and free overflow conditions. Coleman and Smith (1923) stated that minimum nape height over side weirs should not be less than 19 mm because of the surface tension over the weir crest. Therefore, the minimum nape height is taken into account as 20 mm. Thus**,** 'We' number was neglected in the dimensional analysis. The experiments were conducted for the lengths (widths) of the weir (L=0.25, 0.50 and 0.75 m), heights of the weir (p=0.12, 0.16 and 0.20 m), and three types triangular side weir. Type 1 has included angle of 45° and its upstream and downstream crest lengths are equal to each other (Table 1a). Type 2 has upstream sidewall angle of 22.5° and its upstream crest length is equal to one third of upstream crest length at Type 1 (Table 1b). Type 3 has upstream sidewall angle of 22.5° and its upstream crest length is equal to two thirds of upstream crest length at Type 1 (Table 1c). The notations and location of the side weir and the range of test variables are given in Table 1, respectively. Hence, a total of 679 test runs were performed in the current study to determine the discharge coefficient.

EXPERIMENTAL RESULTS AND ANALYSIS

Experiments in this study were conducted to determine the discharge coefficient of triangular labyrinth side weirs with various upstream crest lengths. The discharge coefficient was computed using the De Marchi equation (Equation 1).

It is observed from Figure 3a - 3c that discharge coefficients of labyrinth side weirs have much higher values than those rectangular side weirs. Especially, labyrinth side weir at Type 1 has greater C_d values. The crest length of labyrinth side weir is always longer than that of classical rectangular side weir. Since the weir length is excessive, more intensive secondary flow occur. Thus, intensive secondary flow results with higher flow rate discharge. It is observed from Figure 3(a - c) that C_d values of labyrinth weir for Types 2 and 3 are close to each other. The results indicated that discharge

Table 1. Plan view of the side weirs located on the main channel and their dimensions.

L (cm)	(a) Type 1	(b) Type 2	(c) Type 3
25	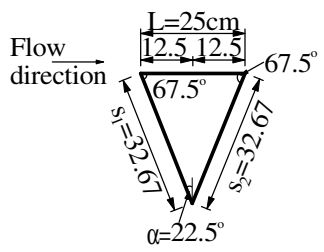 S=S1+S2, S1=S2	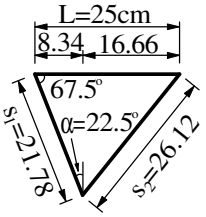 S=S1+S2, S1<S2	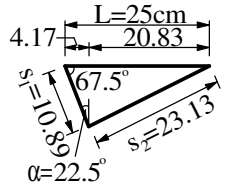 S=S1+S2, S1<S2
50	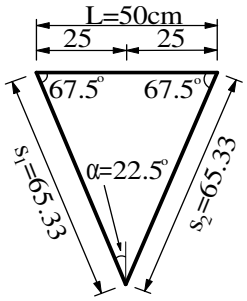 S=S1+S2, S1=S2	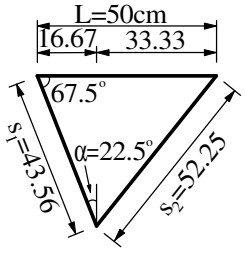 S=S1+S2, S1<S2	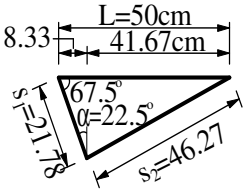 S=S1+S2, S1<S2
75	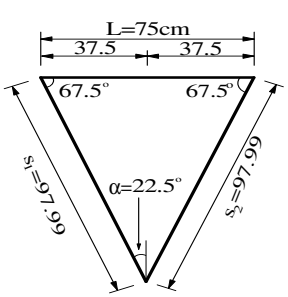 S=S1+S2, S1=S2	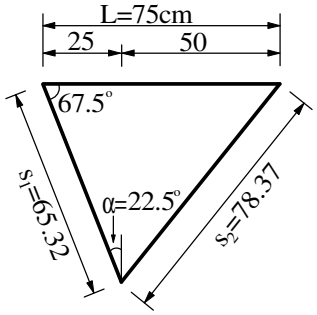 S=S1+S2, S1<S2	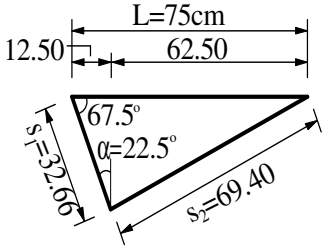 S=S1+S2, S1<S2

coefficient increases when Froude number increases. Emiroglu et al. (2010a, b) and Agaccioglu and Yüksel (1998) also found the similar tendency. The intensity of secondary motion created by lateral flow increases with an increase in the overflow length. An increase in the secondary flow causes the growth of the deviation angle and kinetic energy towards the side-weir when the relative side-weir length increases. Therefore, an increase at the F_1 values also increases C_d values for p/b = 0.40 and L/b = 1.50, as shown in Figure 3(c).

The variation of the discharge coefficient of the side weirs located on the straight channel was investigated for different L/b ratios in Figure 4(a - c). It can be seen that, as the L/b ratio increases, the C_d values also increase. In other words, higher C_d values are obtained at high L/b ratios due to an increase at the intensity of secondary flow created by lateral flow. El-Khashab and Smith (1976) pointed out that the secondary flow condition due to lateral flow is dominant when a side weir is relatively long.

C_d is plotted against F_1, together with different dimensionless weir heights (p/h_1) for the dimensionless weir length L/b = 1.0 in Figure 5. The effect of p/h_1 on the discharge coefficient is very significant for the same Froude number in all the side weir dimensions, and C_d value increases with an increase in p/h_1 values. The effect

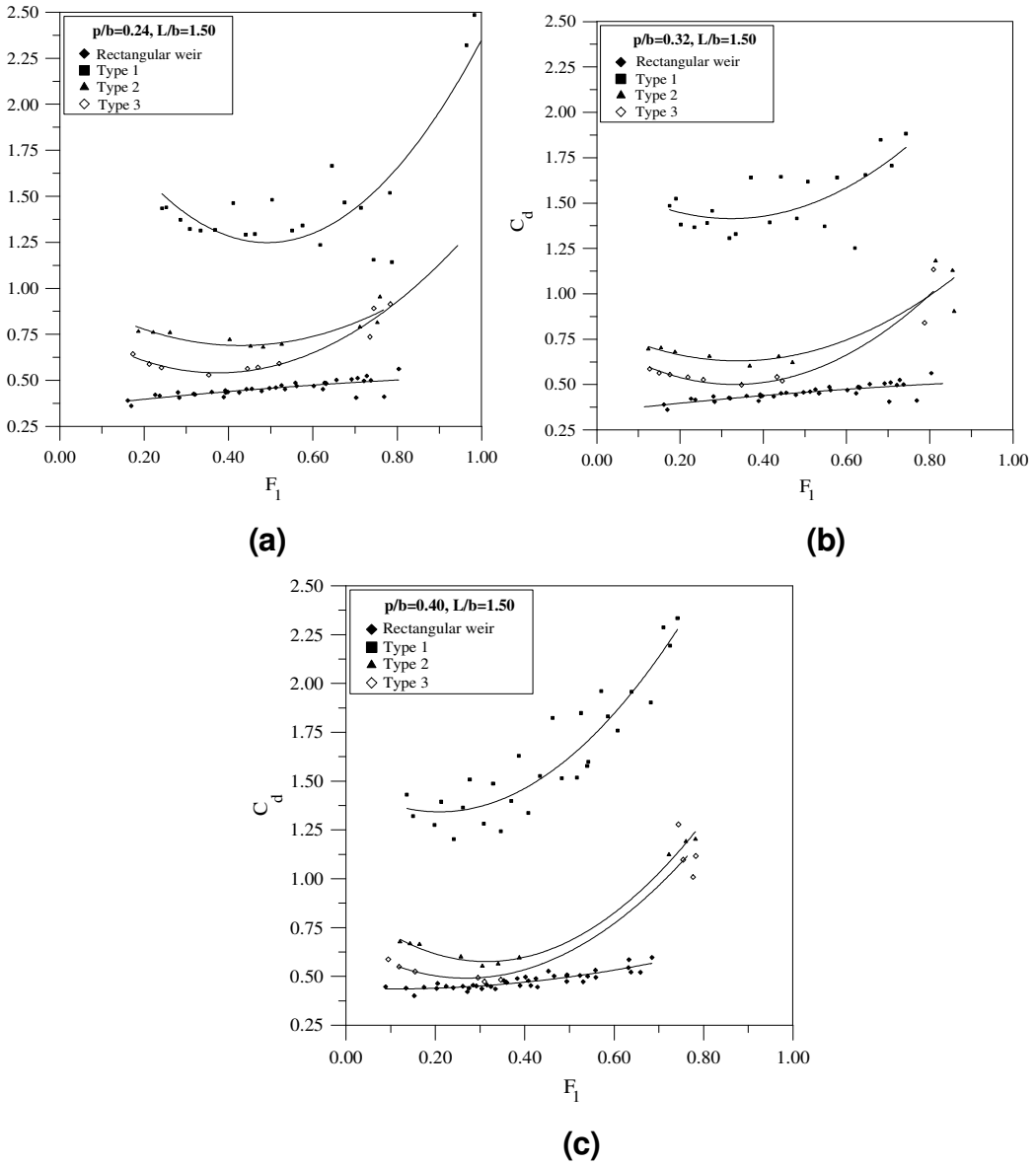

Figure 3 (a-c). C_d for different F_1 values.

of p/h_1 on C_d can be explained by the existence of a discontinuity region. This discontinuity region has a strong secondary motion next to the boundary of the weir-side. The intensity of this secondary motion next to the boundary depends on the crest height of the side weir and decreases with the crest height increase of side weir, due to the friction of the weir surface.

Figure 6 shows that C_d is plotted against F_1 together with different dimensionless weir heights (p/h_1). The p/h_1 value was kept constant and series of experiments with different Froude numbers were taken account of. It can be seen that, C_d increases with increasing p/h_1. The effect of p/h_1 on C_d can be explained with the discontinuity region.

The discharge coefficient values of the labyrinth side weirs tested are compared with those of Subramanya and Awasty (1972), Ranga et al. (1979) and Hager (1987), as shown in Figure 7. Present study data used at the comparison belong to Type 2. Equations presented by Subramanya and Awasty (1972), Ranga et al. (1979) and Hager (1987) are for rectangular side-weirs. As it can be seen in Figure 7, the values of C_d for the labyrinth side weir tested are higher than those of the other works.

Empirical correlations to predict discharge coefficient C_d were developed for triangular side weirs with various upstream crest lengths (that is, Type 1, 2 and 3), according to the result of dimensionless analysis. The

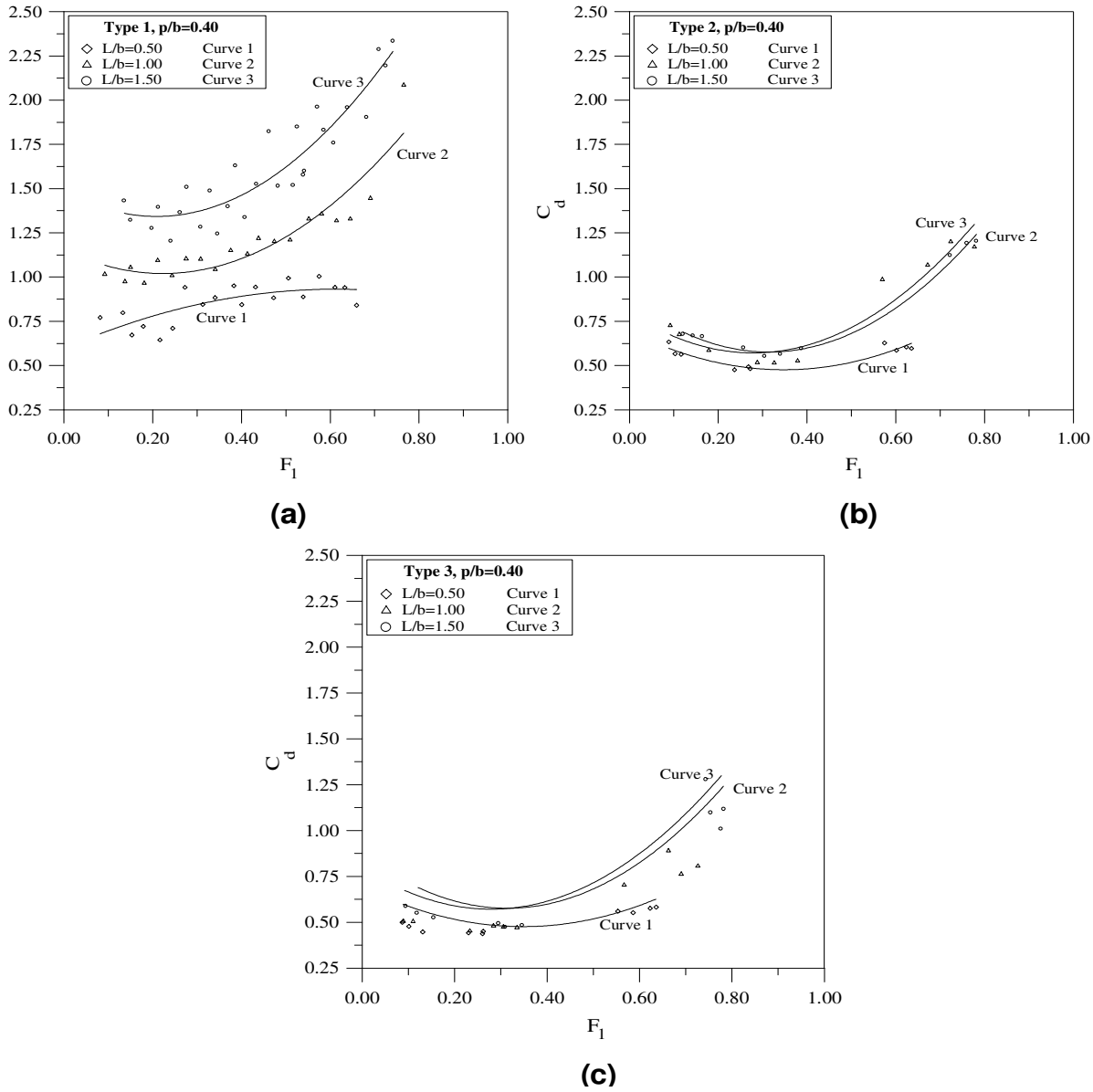

Figure 4. C_d versus different F_1 values for L/b=0.50, 1.00 and 1.50.

resulting correlations are given in Equation 10 – 12:

For Type 1,

$$C_d = 6x10^{-6}\left[5{,}1302 + 0{,}0198\left(\frac{L}{b}\right)^{0{,}9993} + 0{,}3274\left(\frac{L}{s}\right)^{0{,}0411} - 3{,}9153\left(\frac{p}{h_1}\right)^{-0{,}0214} + 0{,}048\,\mathbf{F}_1^{3{,}3687}\right]^{28{,}4053} \quad (10)$$

For Type 2,

$$C_d = 0{,}6753\left[0{,}67828 + 0{,}1791\left(\frac{L}{b}\right)^{0{,}5886} + 0{,}2206\left(\frac{L}{s}\right)^{2{,}8033} + 0{,}2638\left(\frac{p}{h_1}\right)^{4{,}9559} + 0{,}4444\,\mathbf{F}_1^{2{,}9337}\right]^{2{,}0798} \quad (11)$$

For Type 3,

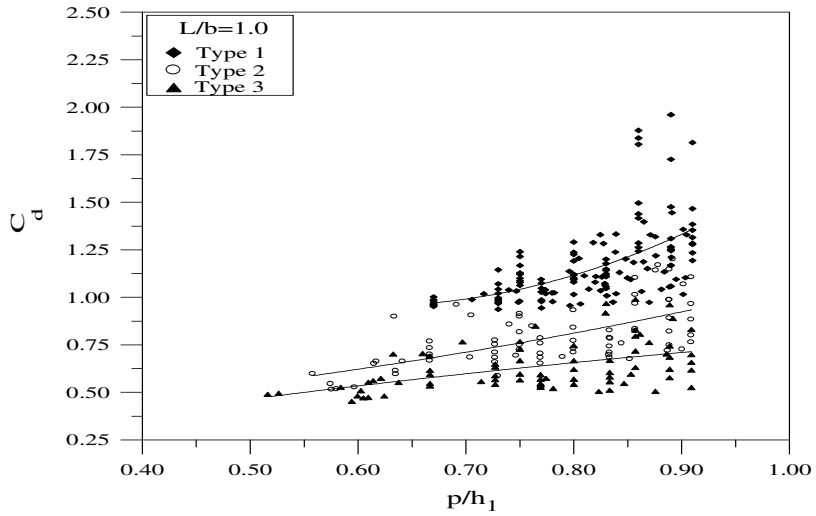

Figure 5. Side weir coefficient (C_d) versus F_1 together with L/b = 1.0.

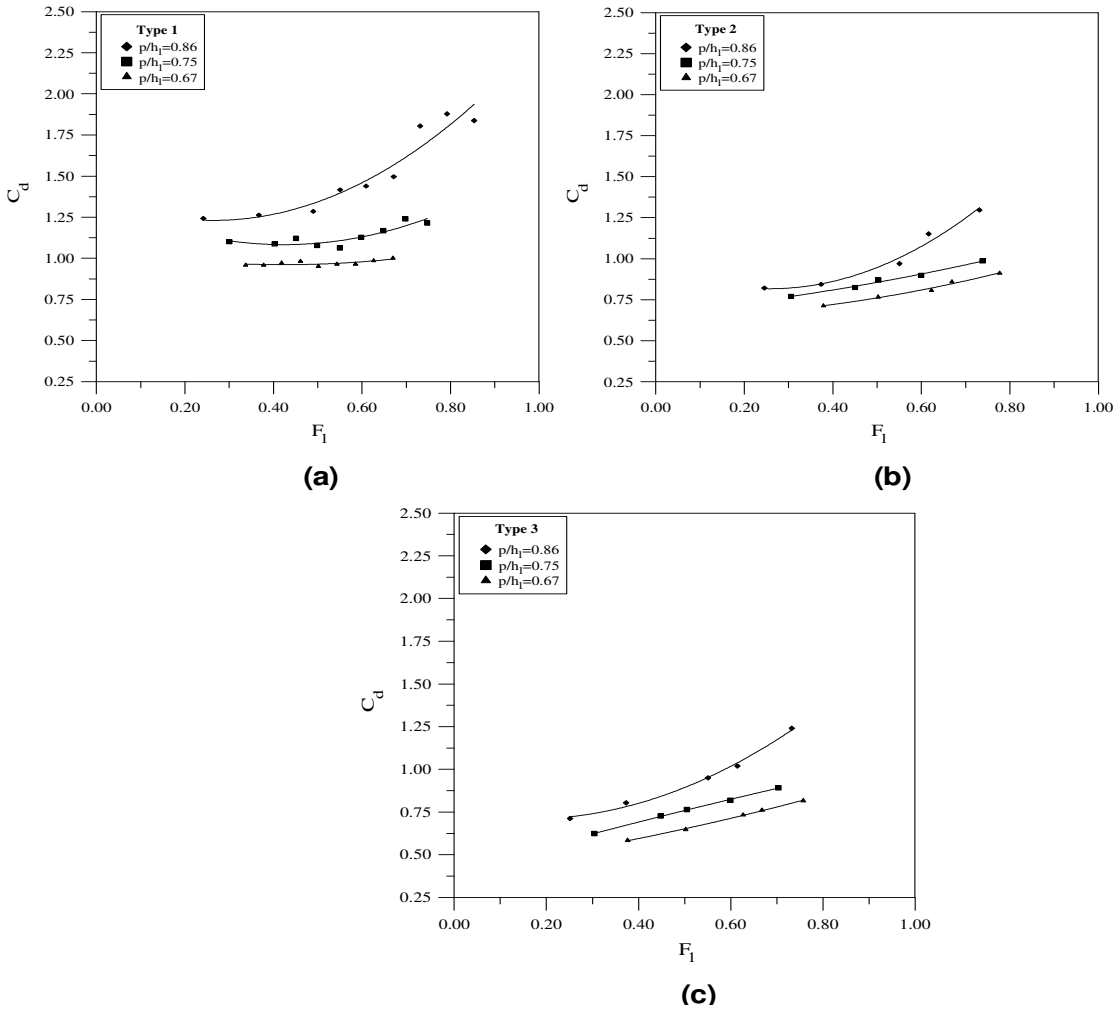

Figure 6. Side weir coefficient (C_d) versus F_1 together with different dimensionless weir heights (p/h_1).

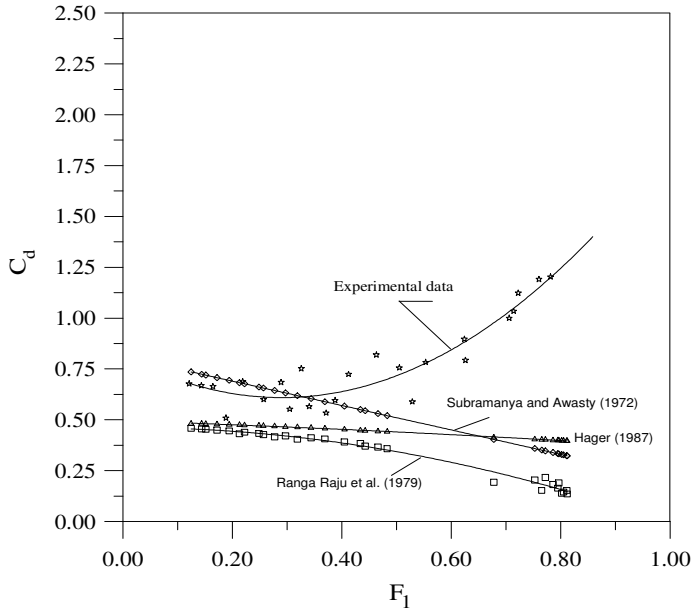

Figure 7. Comparison of the results of present study with the equations of Subramanya and Awasty (1972), Ranga et al. (1979) and Hager (1987).

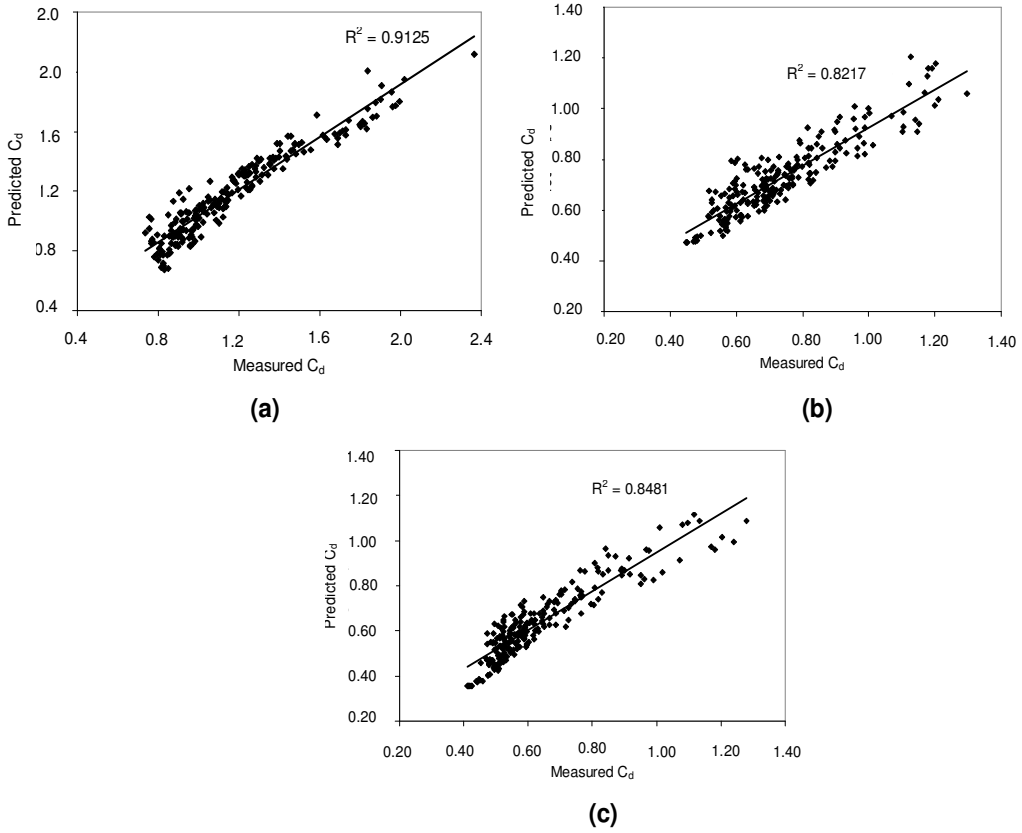

Figure 8. Comparison of discharge coefficient in triangular labyrinth side weirs between observed and calculated values: (a) Type 1, (b) Type 2, (c) Type 3.

$$C_d = 1{,}1489\left[0{,}3007 + 0{,}1791\left(\frac{L}{b}\right)^{0{,}5886} + 0{,}2206\left(\frac{L}{s}\right)^{2{,}8033} + 0{,}2638\left(\frac{p}{h_1}\right)^{4{,}9559} + 0{,}4444\,\mathbf{F}_1^{2{,}9337}\right]^{1{,}7936} \quad (12)$$

where Froude number F_1 is dimensionless, the discharge coefficient C_d is dimensionless, the crest height of the side weir *p,* the width (length) of the side weir *L,* the width of the main channel *b*, the overflow length of side weir *s*, and the depth of flow at the upstream end of the side weir in the main channel centerline h_1 are in meters.

For the 679 data points used, the correlation coefficients for Equations 10, 11 and 12 are 0.95, 0.91 and 0.92, respectively. The observed discharge coefficient values were compared with those calculated with Equations 10, 11, and 12. Good agreements between the observed discharge coefficient values and the values calculated from the predictive equations were obtained. Further confidence in the correlations is seen in Figure 8 (a - c).

Conclusions

In the presented study, the discharge coefficient of triangular labyrinth side weirs with various upstream crest lengths under subcritical flow conditions was investigated. Data from the experimental studies were used to develop equations for estimation of discharge coefficient in triangular labyrinth side weirs having various upstream crest lengths. Accurate equations to calculate the discharge coefficient were obtained. The discharge over these side weirs can be obtained using equations presented in the current study. The results showed that the discharge coefficient of the labyrinth side weir is relatively high when compared with that of the classic side weir. Also, as the dimensionless weir length *(L/b)* ratio increases, the discharge coefficient (C_d) increases. Moreover, it is found that a decrease in upstream crest lengths of the labyrinth side weir causes a considerable decrease in the C_d of the side weir.

ACKNOWLEDGEMENT

The authors are grateful to the Scientific and Technological Research Council of Turkey (TUBITAK) for their financial support.

Notations: ***b,*** Width of channel; ***C_d,*** side weir discharge coefficient (De Marchi coefficient); ***E,*** specific energy in the main channel; **F_1,** Froude number at upstream end of side weir; ***g,*** acceleration due to gravity; ***h,*** main channel depth; ***h_1,*** flow depth at upstream end of side weir at channel center; ***h_2,*** flow depth at downstream end of side weir at channel center; ***L,*** length (width) of side weir; ***s,*** total weir crest length (overflow length); ***s_1,*** upstream crest length of the triangular side weir; ***s_2,*** downstream crest length of the triangular side weir; ***p,*** height of weir crest; ***Q_1,*** discharge at the upstream end of the side weir in the main channel; ***Q_2,*** discharge at the downstream end of the side weir in the main channel; ***Q_w,*** total discharge overflowed the side weir; ***q,*** discharge per unit length over side weir; ***dQ/dx,*** discharge per unit length of side weir; **R,** correlation coefficient; ***x,*** distance along side weir measured from upstream end of side weir; ***V,*** mean velocity in any section of channel; ***V_1,*** mean velocity of flow at the upstream end of side weir; ***V_2,*** mean velocity of flow at the downstream of side-weir; ***V_s,*** velocity of flow dQ_s over the brink; ***θ,*** labyrinth side weir included angle; ***ψ,*** deviation angle of flow.

REFERENCES

Ackers P (1957). A theoretical consideration of side-weirs as storm water overflows. Proc. of the Ice, London, 6: 250-269.

Agaccioglu H, Yüksel Y (1998). Side-weir flow in curved channels. J. Irrig. Drain. Eng., 124(3): 163-175.

Aghayari F, Honar T, Keshavarzi A (2009). A Study of spatial variation of discharge efficient in broad-crested inclined side weirs, Irrig. Drain. 58: 246-254.

Bilhan O, Emiroglu ME, Kisi O (2010). Application of two different neural network techniques to lateral outflow over rectangular side weirs located on a straight channel. Adv. Eng. Softw., 41: 831-837.

Borghei M, Jalili MR, Ghodsian M (1999). Discaharge coefficient for sharp-crested side weir in subcritical flow. J. Hydraul. Eng. 125(10): 1051-1056.

Cheong HF (1991). Discharge coefficient of lateral diversion from trapezoidal channel. J. Irrig. Drain. Eng., 117(4): 321-333.

Coleman, GS, Smith D (1923). The discharging capacity of side weirs. Proc. of the ICE, London, 6: 288-304.

Collings VK (1957). Discharge capacity of side weirs. Proc. Inst. of Civ. Engrs., 6, London, England: 288-304.

Cosar A, Agaccioglu H (2004). Discharge coefficient of a triangular side-weir located on a curved channel. J. Irrig. Drain. Eng. 130(5): 321-333.

De Marchi G (1934). Saggio di teoria de funzionamente degli stramazzi letarali. Energ. Elettr. 11: 849-860.

El-Khashab AMM (1975). Hydraulics of flow over side-weirs. PhD Thesis, Univ. of Southampton, England.

El-Khashab AMM, Smith KVH (1976). Experimental investigation of flow over side weirs. J. Hydraul. Div., Proc., 102(Hy9): 1255-1268.

Emiroglu ME, Kaya N, Agaccioglu H (2010a). Discharge capacity of labyrinth side weir located on a straight channel. J. Irrig. Drain. Eng., 136(1): 37-46.

Emiroglu ME, Kaya N, Ozturk M (2007). Investigation of Labyrinth Side Weir Flow and Scouring at the Lateral Intake Region in a Curved Channel. The Scientific and Technological Research Council of Turkey (TUBITAK), Engineering Science Research Grant Group, Project No: 104M394 [in Turkish]: p. 253.

Emiroglu ME, Kisi O, Bilhan O (2010b). Predicting discharge capacity of triangular labyrinth side weir located on a straight channel by using an adaptive neuro-fuzzy technique. Adv. Eng. Softw., 41(2): 154-160.

Frazer W (1957). The behavior of side weirs in prismatic rectangular

channels. London, England. Proc. Inst. Civ. Engrs., 6: 305-327.
Ghodsian M (2003). Supercritical flow over rectangular side weir. Canadian J. Civil Eng., 30(3): 596-600.
Hager WH (1987). Lateral outflow over side weirs. J. Irrig. Drain. Eng., 113(4): 491-504.
Hager WH (1994). Supercritical flow in circular-shaped side weirs. J. Irrig. Drain. Eng. 120(1): 1-12.
Helweg OJ (1991). Microcomputer applications in water resources. Prentice-Hall, Englewood Cliffs, N.J.
Kumar CP, Pathak SK (1987). Triangular side weirs. J. Irrig. Drain. Eng., 113(1): 98-105.
May RWP, Bromwich BC, Gasowski Y, Rickard CE (2003). Hydraulic design of side weirs. Thomas Telford Publishing, London: p. 133.
Nandesomoorthy T, Thomson A (1972). Discussion of spatially varied flow over side weir. J. Hydroul. Eng., 98(12): 2234-2235.
Oliveto G, Biggiero V, Fiorentino M (2001). Hydraulic features of supercritical flow along prismatic side weirs. J. Hydraul. Res., 39(1): 73-82.
Ranga RKG, Prasad B, Grupta SK (1979). Side weir in rectangular channels. J. Hydraul. Div. Proc., 105(HY5): 547-554.
Singh R, Manivannan D, Satyanarayana T (1994). Discharge coefficient of rectangular side weirs. J. Irrig. Drain. Eng. Proc., 120(4): 814-819.
Subramanya K, Awasthy SC (1972). Spatially varied flow over side weirs. J. Hydraul. Div. Proc. ASCE., 98(HY1): 1-10.
Swamee PK, Santosh KP, Masoud SA (1994). Side weir analysis using elementary discharge coefficient. J. Irrig. Drain. Eng., 120(4): 742-755.
Tullis JP, Nosratollah A, Waldron D (1995). Design of labyrinth spillways. J. Hydraul. Eng., 121(3): 247-255
Uyumaz A, Muslu Y (1985). Flow over side weir in circular channels. J. Hydraul. Eng., 111(1): 144-160.
Yu-Tech L (1972). Discussion of spatially varied flow over side weir. J. Hydraul.Eng., 98(11): 2046-2048.